

SUPPORTING INFORMATION

Catalytic oxidation of diorganosilanes to 1,1,3,3-tetraorganodisiloxanes with gold nanoparticle assembly at water-chloroform interface

Ravi Shankar,^{*a} Asmita Sharma,^a Bhawana Jangir,^a Manchal Chaudhary^a and Gabreile Kociok-Köhn^b

^aDepartment of Chemistry, Indian Institute of Technology Delhi, Hauz Khas, New Delhi-110016.

^bDepartment of Chemistry, University of Bath, Bath BA2 7AY, UK.

**Corresponding Author E-mail:* shankar@chemistry.iitd.ac.in

Index

	Page No.
Fig. S1 Photograph of self-assembly of AuNPs (in PIC-1) stabilized at water-chloroform interface.	3
Fig. S2 X-Ray Photoelectron spectrum of AuNPs.	3
Fig. S3 FESEM and HRTEM micrographs of AuNPs in PIC-1	4
Fig. S4 UV-Vis spectrum of AuNPs in PIC-1 .	4
Fig. S5 GC-MS spectrum of (HMePhSi) ₂ O (1) and MePhSi(OSiMePhH) ₂ .	5
Fig. S6 Kinetic plots for hydrolytic oxidation of MePhSiH ₂ at 25 and 80 °C.	5
Fig. S7 HRTEM image of AuNPs after fourth cycle of hydrolytic oxidation of methylphenylsilane at 80 °C.	6
Fig. S8 GC-MS spectrum of {HMe(<i>n</i> -Hex)Si} ₂ O, 2 .	6
Table S1 Summary of crystallographic data for (HPh ₂ Si) ₂ O, (7).	7
Table S2 Selected bond distances (Angstroms) and bond angles (Degrees) for (HPh ₂ Si) ₂ O, (7).	8
Fig. S9 ORTEP view of molecular structure (with 30 % probability factor) of 7	9

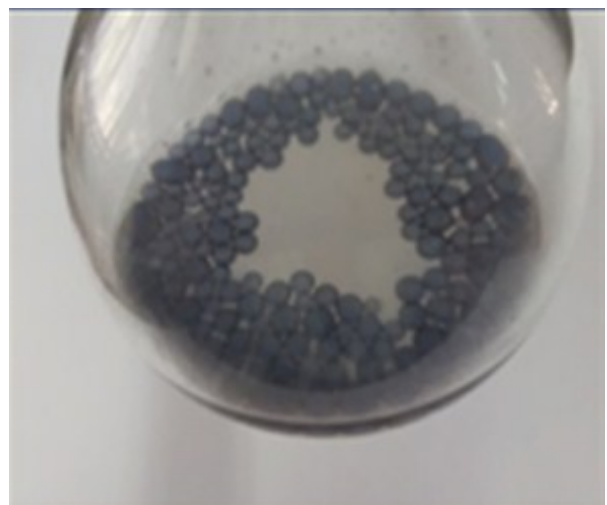


Fig. S1. Photograph of self-assembly of AuNPs (in **PIC-1**) stabilized at water-chloroform interface

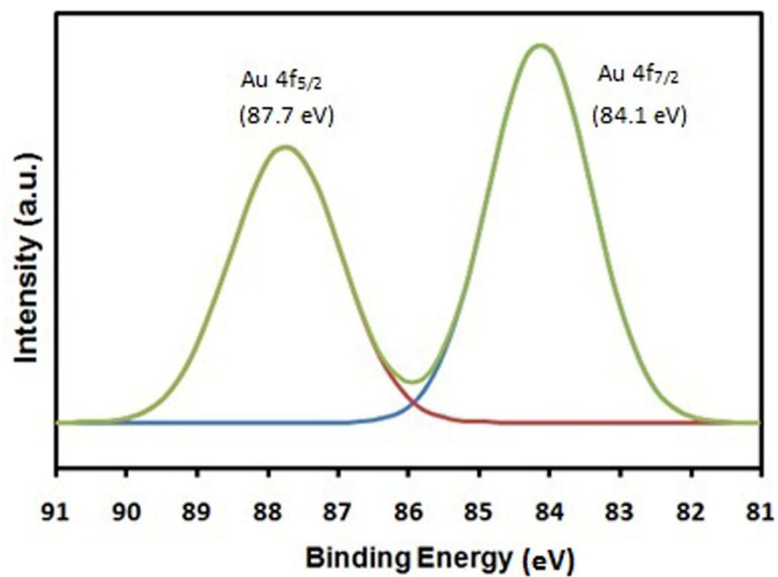


Fig. S2. X-Ray Photoelectron spectrum of AuNPs.

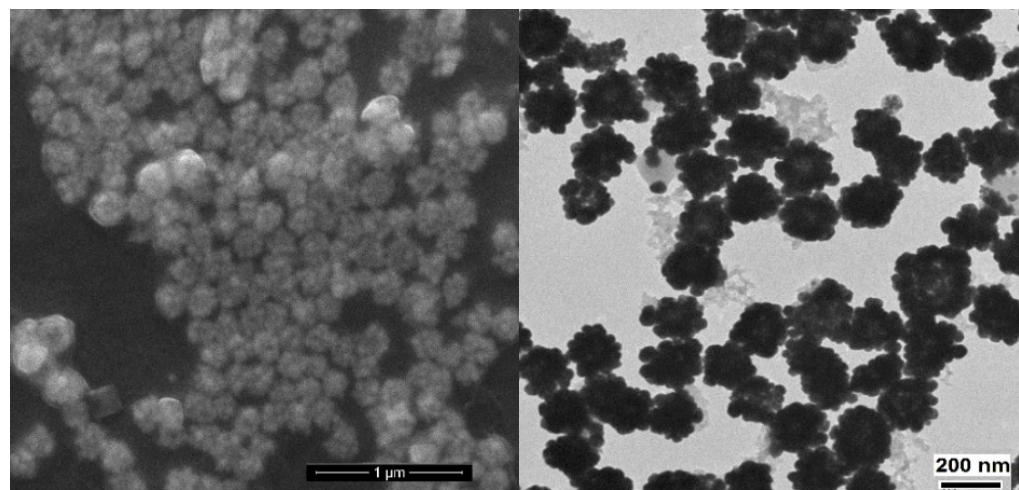


Fig. S3. FESEM and HRTEM micrographs of AuNPs in **PIC-1**.

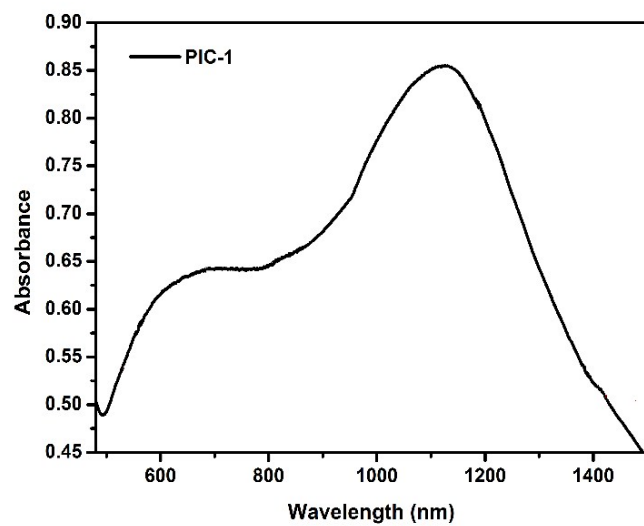


Fig. S4. UV-Vis spectrum of AuNPs in **PIC-1**.

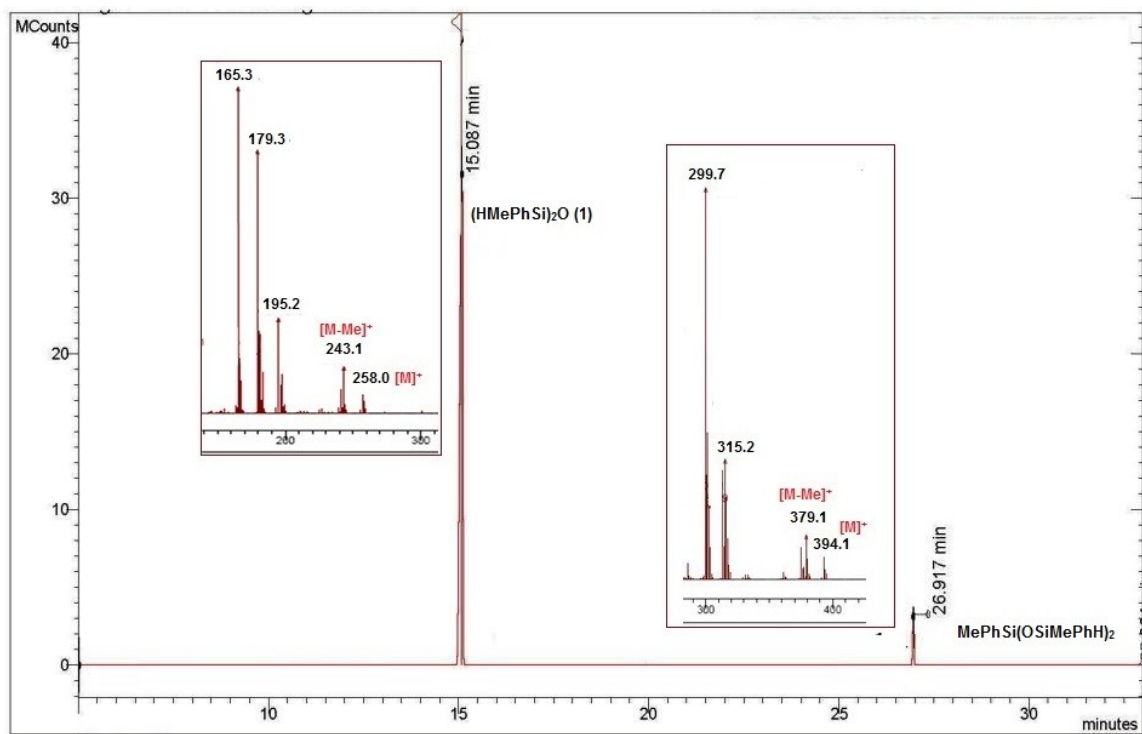


Fig. S5. GC-MS spectrum of $(\text{HMePhSi})_2\text{O}$ (1): $m/z = 258$, $t_R = 15.0$ min and $\text{MePhSi}(\text{OSiMePhH})_2$: $m/z = 394$, $t_R = 26.9$ min.

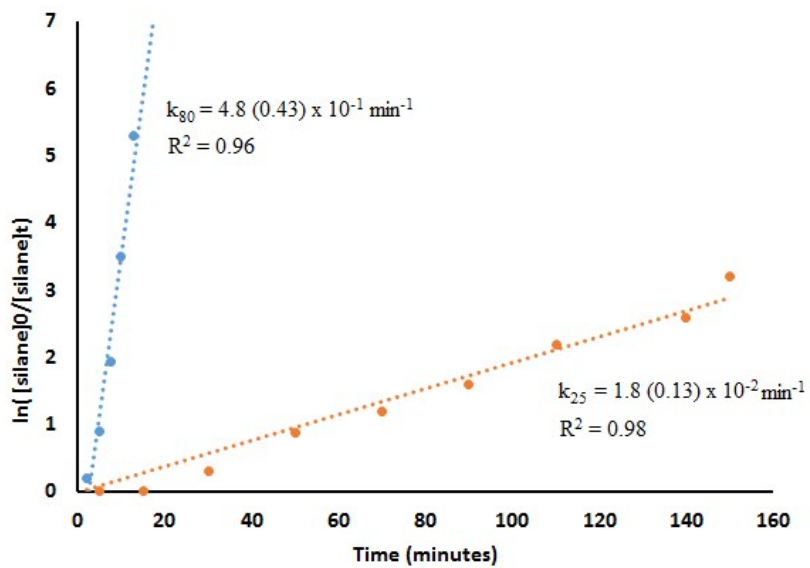


Fig. S6. Kinetic plots for hydrolytic oxidation of MePhSiH_2 at 25 and 80 °C, values in parenthesis represent standard deviation.

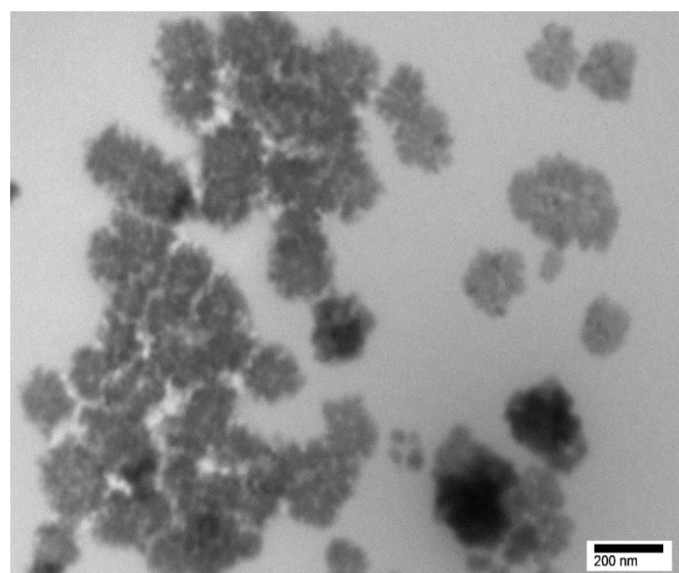


Fig. S7. HRTEM image of AuNPs after fourth cycle of hydrolytic oxidation of methylphenylsilane at 80 °C.

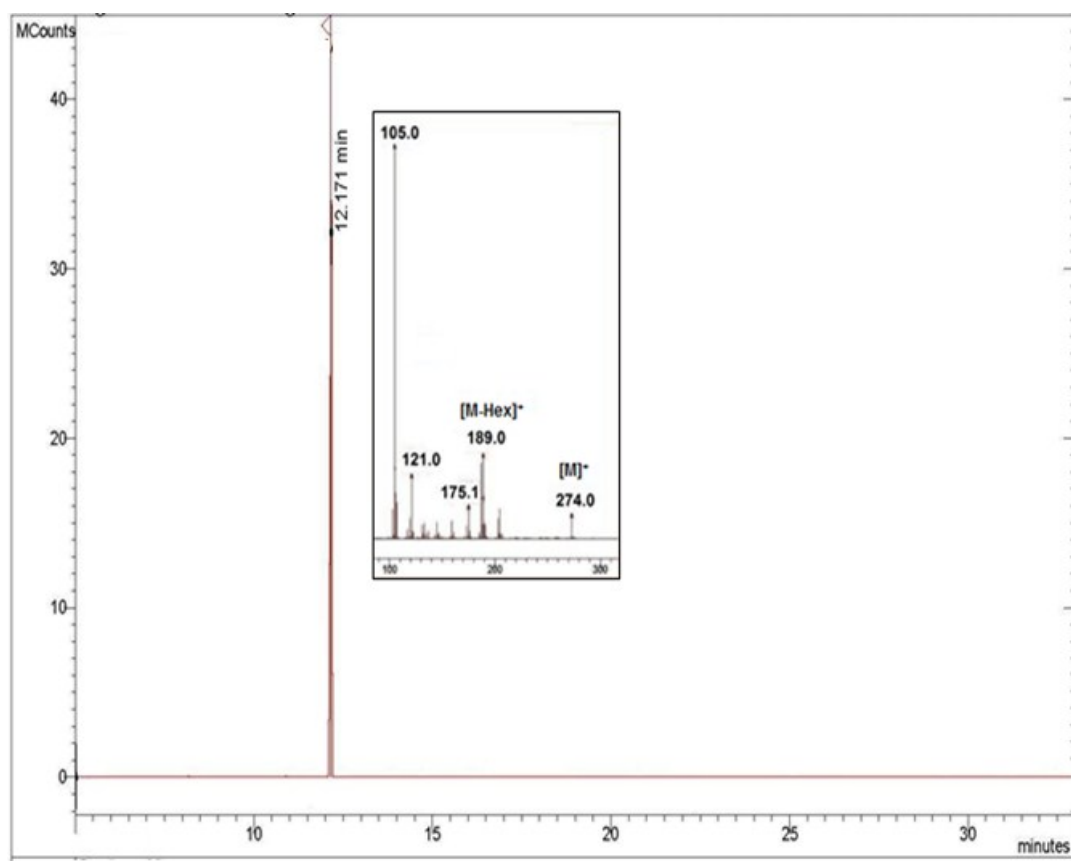


Fig. S8. GC-MS spectrum of $\{\text{HMe}(n\text{-Hex})\text{Si}\}_2\text{O}$, **2**.

Table S1. Summary of crystallographic data for (HPh₂Si)₂O, (7).

Empirical formula	C ₂₄ H ₂₂ O ₁ Si ₂
Formula weight	382.60
Temperature (K)	298(2)
Wavelength (Å)	0.71073
Crystal system	Monoclinic
Space group	P 2 ₁ /n
a, Å	12.567(7)
b, Å	6.088(4)
c, Å	14.018(8)
α, deg	90
β, deg	95.794(16)
γ, deg	90
Volume, Å ³	1067.0(11)
Z	2
ρ calcd. (mg/m ³)	1.191
μ (mm ⁻¹)	0.177
F(000)	404
Crystal size (mm ³)	0.43 x 0.33 x 0.22
Theta range for data collection (deg)	2.075 to 25.992
Index range	-15<=h<=13, -7<=k<=7, -17<=l<=17
Reflections collected	15339
Independent reflections	2107
Absorption correction	Semi-empirical from equivalents
Max. and min. transmission	0.768 and 0.626
R(int)	0.0460
Refinement method	Full-matrix least-squares on F ²
Data / restraints / parameters	2107 / 8 / 202
Goodness-of-fit on F ²	1.050
Final R indices [I>2σ(I)]	R1 = 0.0429, wR2 = 0.1200
R indices (all data)	R1 = 0.0749, wR2 = 0.1428
Largest diff. peak and hole (e.Å ⁻³)	0.146 and -0.183 e.Å ⁻³
CCDC number	1871681

Table S2. Selected bond distances (\AA) and bond angles ($^\circ$) for $(\text{HPh}_2\text{Si})_2\text{O}$, (7).

C(1A)-Si(1A)	1.857(5)
C(1B)-Si(1B)	1.860(5)
C(7A)-Si(1A)	1.866(5)
C(7B)-Si(1B)	1.870(5)
O(1)-Si(1A)	1.615(4)
O(1)-Si(1B)	1.604(5)
Si(1A)-H(1A)	1.45(3)
Si(1A)-O(1)-Si(1B)	162.2(4)
O(1)-Si(1A)-C(1A)	110.1(5)
O(1)-Si(1A)-C(7A)	109.9(4)
O(1)-Si(1B)-C(1B)	108.7(5)
O(1)-Si(1B)-C(7B)	108.4(4)
C(1A)-Si(1A)-C(7A)	103.9(6)
C(1B)-Si(1B)-H(7B)	118.6(6)

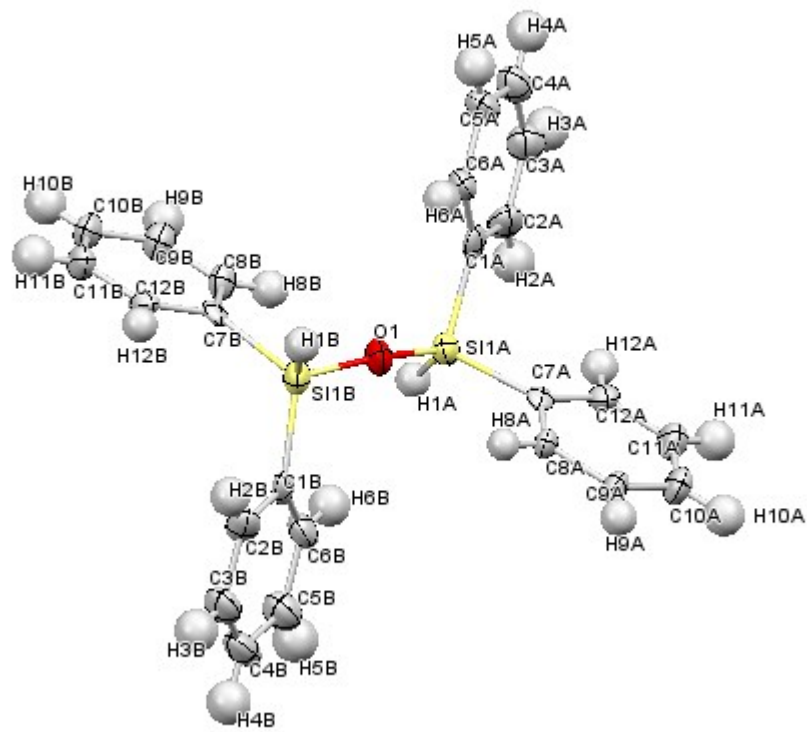


Fig. S9 ORTEP view of molecular structure (with 30 % probability factor) of **7**. Selected bond lengths (\AA) and angles ($^\circ$): Si1A-O1 = 1.615(4), Si1B-O1 = 1.604(5), Si1A-O1-SiB = 162.2(4).